

Effect of thermal curing on the properties of thin films based on benzophenonetetracarboxylic dianhydride and 4,4'-diamino-3,3'-dimethyldiphenylmethane

Ion Sava · Ștefan Chișcă · Maria Brumă ·
Gabriela Lisa

Received: 18 August 2010 / Accepted: 12 January 2011 / Published online: 12 February 2011
© Akadémiai Kiadó, Budapest, Hungary 2011

Abstract The processing of polyimide films from polyamidic acid solutions involves the simultaneous loss of solvent and chemical conversion, and may imply structural reorganization such as orientation or crystallization. The effect of thermal treatment on the thermal, mechanical and dielectric properties of polymer films based on benzophenonetetracarboxylic dianhydride and 4,4'-diamino-3,3'-dimethyl diphenylmethane have been investigated. The thermal treatment of polyamidic acid at different temperatures led to compounds with different degree of imidization; it turned out that the imidization process took place with high speed until 240 °C and then remained constant. The dynamic mechanical analysis (DMA), contact angles, and dielectric measurements revealed that the storage modulus and contact angles increased with increasing of curing temperature while the dielectric constant decreased.

Keywords Polyamidic acids · Thermal treatment · Thin films · Dynamic mechanical analysis

Introduction

Aromatic polyimides generally have excellent thermal, mechanical, and electrical properties primarily because of their heterocyclic structure [1–6]. However, even higher

thermal stability and mechanical strength than those of pure polyimides are sometimes required for special applications. The fabrication of polyimide nanocomposite systems, such as hybrids with organoclays, mesoporous silica is a new approach to obtain materials with improved properties [7–9]. The use of polyimides as dispersants for carbon nanotubes, in which nanotubes are homogeneously dispersed in the polyimide matrix, has also been studied [10, 11]. Detailed investigations of the thermal imidization reactions and structural evolution of pure polyimides are still required if we are to fully understand and utilize the “processing–structure–property relationship” in the design of further polyimide systems for high performance applications.

In order to obtain polyimides, poly(amic acid) (PAA) or poly(amic dialkyl ester) (PAE) is synthesized as a precursor polymer. These precursor polymers contain carboxylic and amide linkages which are soluble in polar organic solvents and thin films can be obtained by the simple spin casting of their solutions. The precursor films are then thermally converted to polyimides, a process that involves ring closing reactions. One shortcoming of PAA as a precursor is the instability of its solutions, i.e., its tendency to spontaneously decompose due to hydrolysis and exchange reactions. As a result, there is a rapid drop in solution viscosity, especially at elevated temperatures. PAE precursors have some advantages over PAA, in spite of their relatively complicated synthesis pathways; in particular, they have better solution properties and hydrolytic stability due to the absence of carboxylic acid groups that cause monomer-polymer equilibration in solution [12–16]. Many studies focus on the thermal imidization of polyamidic acid but less of them show the influence of the curing temperature on properties of partially imidized polymers [17, 18]. It is particularly interesting to study the influence of the

I. Sava (✉) · Ș. Chișcă · M. Brumă
“Petru Poni” Institute of Macromolecular Chemistry, Aleea Gr.
Ghica Voda 41 A, 700487 Iasi, Romania
e-mail: isava@icmpp.ro

G. Lisa
Faculty of Chemical Engineering and Environmental Protection,
Department of Chemical Engineering, “Gh.Asachi” Technical
University Iasi, Bd. Mangeron 71, 700050 Iasi, Romania

surface polarity determined by the presence of polar COOH and amide groups on the properties of partially imidized polyamic acids as compared with those of the resulting polyimides, during different steps of thermal treatment. Usually, the polarity of the surface influences the dielectric properties and the contact angle values. In this context the goal of the paper is to present the effect of thermal treatment on the thermal, mechanical and dielectric properties of polymer films based on benzophenonetetracarboxylic dianhydride and 4,4'-diamino-3,3'-dimethyl diphenylmethane. Previously, we reported only the synthesis of polyimides based on diamines containing flexible methylene bridges, such as 4,4'-diaminodiphenylmethane or 4,4'-diamino-3,3'-dimethyl diphenylmethane and various aromatic dianhydride [19, 20]. Hitherto, to our knowledge, there are no published reports about the curing temperature influence on their above mentioned properties.

Experimental

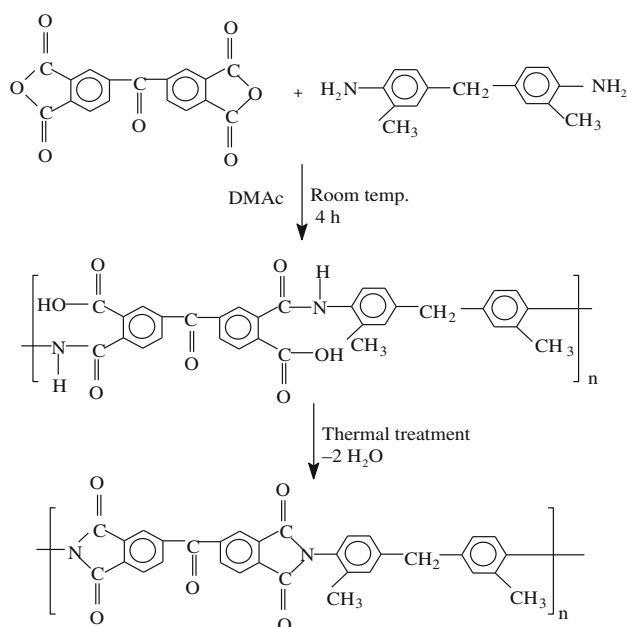
Preparation of the polyimide films

The polymer precursor, polyamic acid (PAA), was synthesized by the reaction of benzophenonetetracarboxylic dianhydride (BTDA) and 4,4'-diamino-3,3'-dimethyldiphenylmethane [21] in *N,N*-dimethylacetamide (DMAc), in 15% solids concentration, by a method previously described [19]. In a typical synthesis (Scheme 1), 4,4'-diamino-3,3'-dimethyl-diphenylmethane was dissolved in DMAc, and an equimolar amount of benzophenonetetracarboxylic dianhydride was added under stirring which was continued for 4 h at room temperature, resulting in a viscous yellow solution. The precursor film was obtained by casting the afore-mentioned homogeneous solution onto glass plates and drying at 100–110 °C over 4 h to evaporate the solvent. The subsequent heating of the precursor films at 150, 180, 210, 240–250, 260–280 °C, consecutively (for 40 min at each temperature) resulted in the final polyimide (PI) films.

The sample of polymer film obtained by casting DMAc polyamic solution on a glass substrate and evaporating solvent in an oven at 110 °C for 4 h was abbreviated **A**. By the thermal treatment of the polymer sample **A** at different temperatures and times we have obtained the other polymer samples which have been investigated in this study. Table 1 presents the conditions of thermal treatment and the abbreviations of the polymer films.

Measurements

FTIR spectra were recorded with a FT-IR VERTEX 70 (Bruker Optics Company), with a resolution of 0.5 cm⁻¹.



Scheme 1 Synthesis of polyimide

Thermogravimetric analysis (TG) of the polymers was performed with a Mettler Toledo 851^e instrument, operating at a heating rate of 10 °C/min, in nitrogen. The polymer samples of 3–5 mg were loaded in alumina crucible and then nonisothermally heated from ambient temperature to 900 °C. For each sample, two reproducible experiments were carried out. Differential scanning calorimetry (DSC) analysis was performed using a Mettler Toledo DSC 1 (Mettler Toledo, Switzerland) operating with version 9.1 of STAR^e software. The samples (2–4 mg) were encapsulated in aluminium pans having pierced lids to allow escape of volatiles. The heating rates of 10 °C min⁻¹ and nitrogen purge of 100 mL min⁻¹ were employed. Dynamic mechanical analysis (DMA) experiments were performed on the polymer film specimens (20 mm long, 10 mm wide, and 30–40 μm thick) on a PerkinElmer Diamond apparatus provided with a standard tension attachment at a heating rate of 2 °C/min in nitrogen atmosphere. Dielectric measurements of the polymer films were performed using an experimental set-up from Novocontrol at various temperatures (in the range of 173–473 K) and frequencies (in the range of 10⁻¹–10⁴ Hz) in a nitrogen atmosphere. The system was equipped with Alpha high resolution dielectric analyzer, the impedance analyzer HP 4191A and temperature controller Quatro version 4.0. Silver electrodes with 20 mm diameter were painted on both samples surfaces to assure a good ohmic contact. Polyimide films with thicknesses comprised between 30 and 50 μm were placed between two round electrodes and tested. Dynamic contact angles were performed by the Wilhelmy plate technique using a Sigma 700 precision tensiometer produced by KSV

Table 1 The conditions of obtaining the polymer samples A–H

Polymer samples	Curing temperature/°C	Polymer samples	Curing temperature/°C
A	110 (240 min)	E	240–250 (40 min)
B	150–160 (40 min)	F	250–260 (100 min)
C	180–185 (40 min)	G	250–260 (270 min)
D	210 (40 min)	H	260–280 (90 min)

instruments. The samples dimensions were 50×10 mm. The rate of immersion-emersion in water was 5 mm min^{-1} , immersion depth being of 5 mm in standard conditions. All measurements were the average of three contact angles values of samples.

Results and discussion

FTIR results

The amide linkages in polyamidic acid have been found to form complexes with residual solvent and other amidic acid groups via both intra- as well as intermolecular hydrogen bondings. In the heating process, the molecules of residual solvent are removed continuously with increasing temperature. Furthermore, the hydrogen bonds weaken with increasing temperature because they are in equilibrium with their constituents [22].

FTIR spectra (Fig. 1a) illustrates the effect of curing temperature on the chemical structure of the polymer samples. The absorption peak at 1778 cm^{-1} , which corresponds to the C=O symmetrical stretching of polyimide, could be observed at $110 \text{ }^\circ\text{C}$. It means that the film starts to imidize at this low temperature. Other authors have also reported the starting of imidization process at low temperature ($87 \text{ }^\circ\text{C}$) [23]. In the same time, the absorption peaks at 1716 cm^{-1} (imide II: C=O asymmetric stretch), 1370 cm^{-1} (imide III: C–N stretching vibration) and 730 cm^{-1} (imide IV: bending vibration of cyclic C=O) are also present [24, 25]. On the other hand, the characteristic absorption bands of amide groups are evidenced at 1600 cm^{-1} (amide I: CNH stretching vibration which in part overlaps with C=C quadrant stretch of the aromatic rings) at 1660 cm^{-1} (amide II: vibration of C=O in the CONH group) and around 3290 cm^{-1} (amide III: COOH and NH_2 vibration). The intensities of the characteristic absorption bands of amidic acid groups decrease drastically with increasing temperature (210 and $260 \text{ }^\circ\text{C}$, respectively) while the characteristic absorption peaks of the imide rings become stronger with increasing temperature. As the curing proceeds, the amide groups are consumed and the residual solvent is driven off (Fig. 1b); the intensities of the

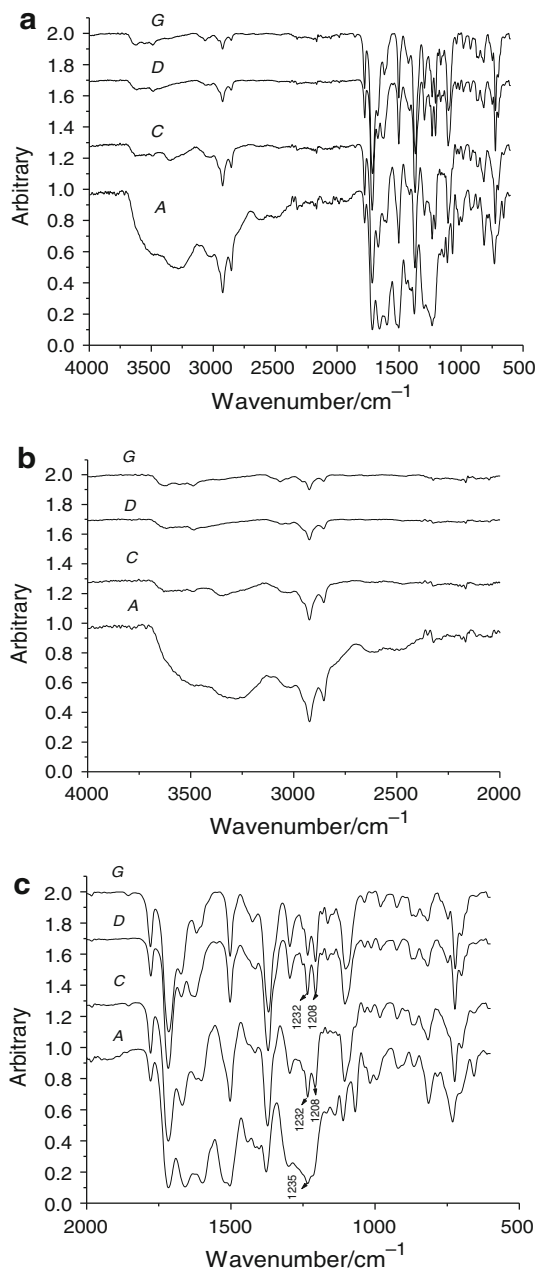


Fig. 1 a FTIR spectra of the polymer samples A, C, D, and G in the range of $4000\text{--}500 \text{ cm}^{-1}$. b FTIR spectra of the polymer samples A, C, D, and G in the range of $4000\text{--}2000 \text{ cm}^{-1}$. c FTIR spectra of the polymer samples A, C, D, and G in the range of $2000\text{--}500 \text{ cm}^{-1}$

absorption bands in the region of 2925 and 2856 cm^{-1} (corresponding to the asymmetric stretching of aliphatic group C–H) decrease.

In the FTIR domain of 800–1250 cm^{-1} (Fig. 1c), the absorption bands varied with the curing temperature. Thus, at low temperature (110 $^{\circ}\text{C}$), the band around 1235 cm^{-1} corresponding to the absorption of $(\text{CO})_2\text{NC}$ imide groups is relatively weak. At 150 $^{\circ}\text{C}$, two well-defined peaks (1232 and 1208 cm^{-1}) appeared and their intensities increase as the cure temperature increases. This phenomenon can be associated with increasing of amount of $(\text{CO})_2\text{NC}$ imide groups. Similar results were reported in the literature for other aromatic polyimides [17]. Moreover, from Fig. 2, where is plotted $\text{C}=\text{O}/\text{C}=\text{C}$ ratios versus temperature, one may observe that the imidization process proceeds with high speed until 240 $^{\circ}\text{C}$ after which it becomes constant. This means that the most of imidization process takes place at this temperature. These ratios have been calculated from the ratio of absorbance at 1778 cm^{-1} for different temperatures (which corresponds to $\text{C}=\text{O}$ symmetrical vibration), to that at 1500 cm^{-1} (taken as standard absorption band for aromatics).

Thermal characterization

Other supporting evidences for the transformations which these materials undergo under thermal treatment (the temperature domains of cyclodehydration reaction, and the thermal stability and thermal decomposition of PI) have been obtained by TG. Usually, the boiling temperature of the solvents containing PAA are relatively high, hence the cyclization reaction of PI from precursor PAA involves simultaneous imidization, evaporation of solvent and crystallization [26–28]. Figure 3 shows TG thermogram and its first derivative performed with PAA film (A) containing residual solvent DMAc. Since the NH and COOH groups in PAA molecular chain easily form hydrogen

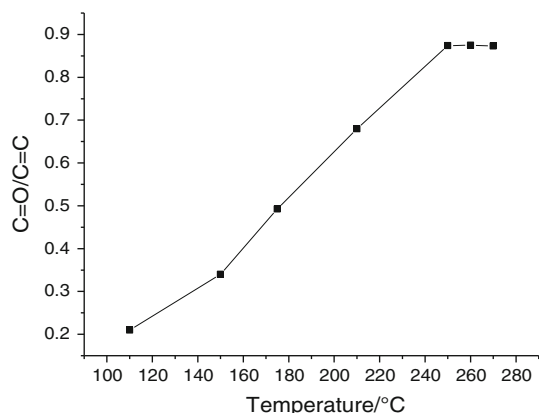


Fig. 2 The dependence of the ratio $\text{C}=\text{O}/\text{C}=\text{C}$ versus cure temperature

bonds with water molecules leading to the moisture absorption, the TG curve shows a slight mass loss (about 1%) below 100 $^{\circ}\text{C}$ due to the release of absorbed water and possible residual solvent. The PAA presents a three-step mass loss behavior below 430 $^{\circ}\text{C}$. The first step appears below 130 $^{\circ}\text{C}$ and involves a relatively small mass loss. This step can be attributed to the decomplexation of DMAc molecules bound to the carboxylic groups and amide linkages of the PAA precursor chains via hydrogen bonding. The second step occurs in the range of 130–273 $^{\circ}\text{C}$ and involves a large mass loss at a high speed. This prominent mass loss is most likely due to the removal of residual solvent and of water formed as byproduct during imide-ring closures in PAA polymer chains being imidized. The highest rate of mass loss determined from DTG appears at 177 $^{\circ}\text{C}$, as the minimum of this curve. The third step occurs over the range of 273–430 $^{\circ}\text{C}$ and involves a very small mass loss with a slow speed, which can be ascribed to the dehydration of partially imidized precursor chains that are still undergoing imide ring closure with a slow imidization rate at the last stage. The TG curve starts to fall at 300 $^{\circ}\text{C}$, the decline having a gentle slope. At temperatures higher than 470 $^{\circ}\text{C}$, another significant mass loss occurs. This mass loss is due to the starting of decomposition of the imidized polymer chains. The maximum rate of decomposition at 560 $^{\circ}\text{C}$ is revealed by the pronounced decrease in mass loss as well as by the presence of a sharp peak in DTG curve. Finally, the TG curve shows a very slight decrease after 700 $^{\circ}\text{C}$.

From the TG and DTG curves in Fig. 4 (for the polymer samples A, B, D, E and H chosen for the readership clarity) and the thermal characteristics of all investigated polymer samples collected in Table 2, one may notice that in the first step there are not significant differences in the mass loss for all the polymer samples. On the other hand, it can be mentioned that in the second step, the T_{onset} (temperature corresponding to the starting degradation step) gradually increases as the cure temperature is increased (Fig. 4). Thus, T_{onset} is 161 $^{\circ}\text{C}$ for the polymer sample

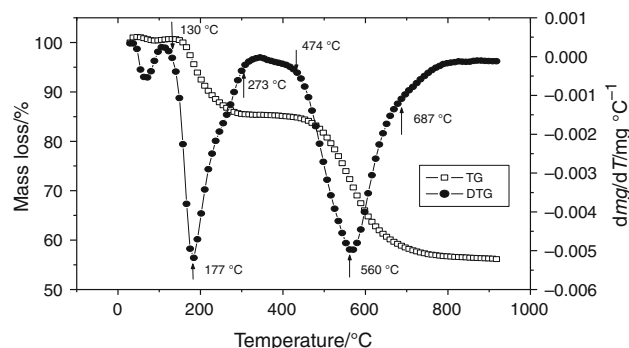


Fig. 3 TG thermogram and its first derivative for polymer sample A

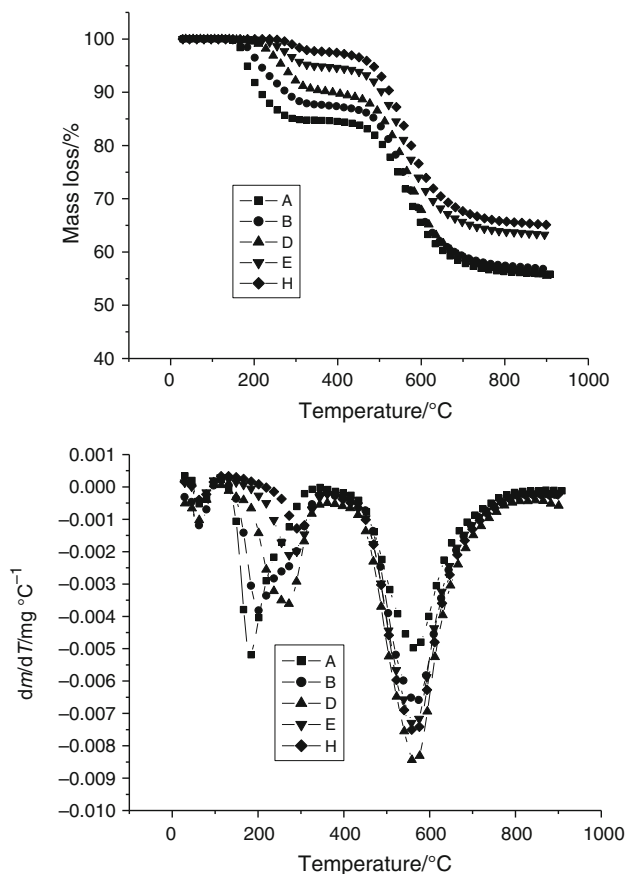


Fig. 4 TG (up) and DTG (bottom) curves of the polymer samples A, B, D, E, and H

A and above 260 °C for polymer samples F, G, and H. In the same time, the mass loss gradually decreases from 15% for polymer sample A until around 2% for polymer samples F, G, and H. The temperature of maximum decomposition rate increases from 177 °C for polymer sample A to 297 °C in the case of polymer sample G. This stage corresponds to the imidization process accompanied by removal of residual solvent. The last stage shows that it is not a big difference between the investigated polymer samples. All the samples start to decompose in the range of 470–490 °C; the temperature of maximum decomposition rate is in the range of 560–570 °C. The mass loss is in the range of 29–35%. This stage corresponds to the decomposition of the imidized polymer chains.

The imidization reaction in solid state depends on the temperature and has a very little relation with time. As can be seen in Fig. 5 there is no any clear transformation in the TG curve if the polymer samples are thermally treated for different time at the same cure temperature (samples F and G with 100 min and 270 min, respectively). In the same time, if the polymer samples C and D are thermal treated at 180 and 210 °C, respectively, for 40 min, the TG curves are almost unchanged, which means that no major

Table 2 Thermal properties of the polymer samples A–H

Polymer samples	Stage of thermal degradation	$T_{\text{onset}}/^\circ\text{C}$	$T_{\text{max}}/^\circ\text{C}$	$T_{\text{endset}}/^\circ\text{C}$	W/%
A	I	55	64	89	0.66
	II	161	177	273	15.38
	III	474	560	687	29.11
B	I	48	62	90	0.89
	II	172	196	302	12.51
	III	494	564	655	30.51
C	I	44	60	90	0.81
	II	182	234	310	9.22
	III	482	567	688	30.04
D	I	47	54.5	82	0.88
	II	198	272	298.5	9.81
	III	477	569.5	679	34.63
E	I	49	61	98	0.48
	II	240	280.5	320	5.32
	III	473	568.5	702	31.75
F	I	47	55	90	0.52
	II	260	284	316	1.69
	III	483	569	708	34.85
G	I	46	59	91	0.61
	II	284	297	325	1.86
	III	467.5	567	737	32.27
H	I	45	62	95	0.45
	II	287	296.5	331	2.71
	III	478	565.5	709	32.61

T_{onset} temperature corresponding to the starting degradation step, T_{max} temperature corresponding to the maximum rate of the degradation process, T_{endset} temperature corresponding to the end of the step, W weight loss

transformations take place in this temperature domain. By increasing the cure temperature at 280 °C (polymer sample H) for 90 min., the TG and DTG curves of the polymer sample did not show visible modification comparing with polymer samples F and G. This can be due to the fact that the imidization degree attains a maximum value at 240–250 °C.

Dynamic mechanical analysis

Dynamic mechanical analysis describes the response of a polymer material to small amplitude cyclic deformation as a function of frequency or temperature. Figure 6 shows the thermal transition behavior of the polymer samples at constant frequency (1 Hz). The storage modulus (E') exhibits a plateau at low temperatures for all the polymer samples; the magnitude of E' is over 10^9 Pa, which is typical for glassy polymers. In this high modulus region, named “glassy”, the segmental mobility is restricted

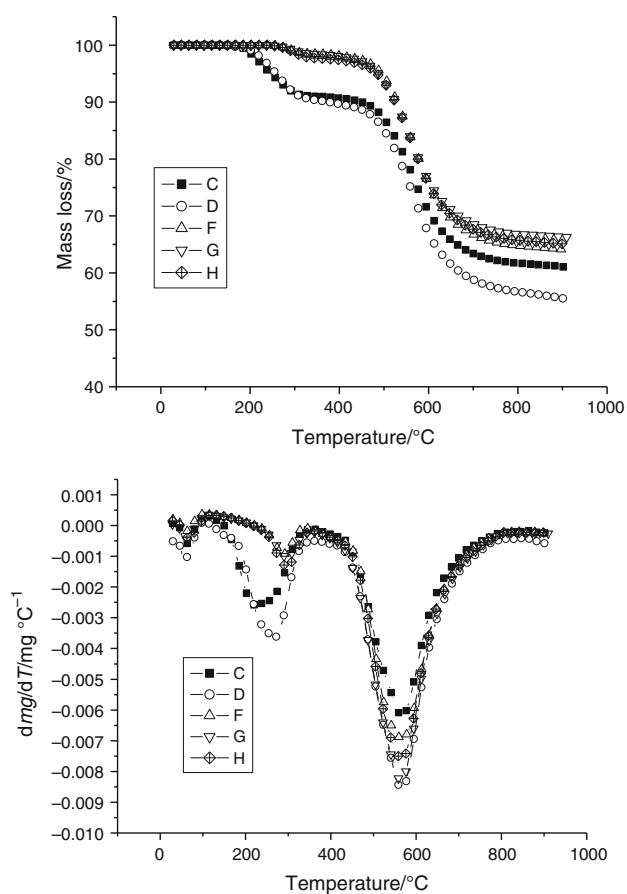


Fig. 5 TG (up) and DTG (bottom) curves of the polymer samples **C**, **D**, **F**, **G**, and **H**

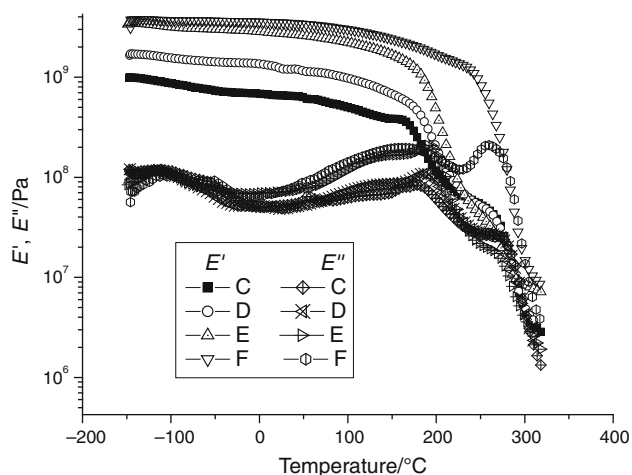


Fig. 6 Storage modulus (E') and loss modulus (E'') of the polymer samples **C**, **D**, **E**, and **F** at a frequency of 1 Hz

[29–31]. The effects of temperature curing on the storage modulus and loss modulus (E'') at a frequency of 1 Hz are seen in Fig. 6.

Thermal imidization is an intramolecular cyclization and for this reason the polymer chain gradually loses the

flexibility as the imidization gets forward. The resulted polyimide is obviously more rigid than the PAA precursor. In the glassy region the E' value recorded at room temperature increases gradually from 0.65×10^9 Pa for polymer samples **C**, 1.2×10^9 Pa for **D**, 2.8×10^9 Pa for **E**, and 3.55×10^9 Pa for **F** (Table 3). The increased values of the storage modulus of the polymer films can be due to the increasing rigidity of the polymer samples as the imidization degree increases.

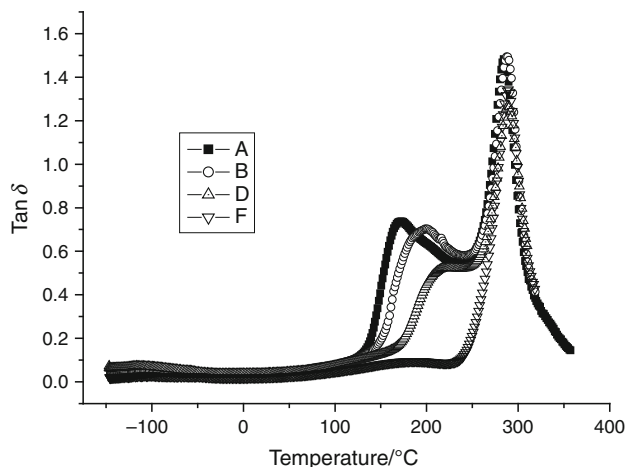
The drops in E' curves and the peaks of E'' and $\tan \delta$ plots report on the physical transitions in polymers. Usually, the transition temperatures are taken at the maximum rate of turndown of the storage modulus E' or at the maxima loss modulus E'' and $\tan \delta$ peaks. In addition, the loss modulus E'' peak appears always at a lower temperature than the $\tan \delta$ peak [17, 18]. The effect of curing on the viscoelastic behavior of the polymer samples can be examined by observing comparatively the tendency of all curves. For more clarity, only $\tan \delta$ of polymer samples **A**, **B**, **D**, and **F** with isothermal curing are presented in Fig. 7. The DMA curve for polymer sample **A**, recorded during the dynamic scanning testing with a heating rate of $2^\circ\text{C}/\text{min}$, indicated a simultaneous evaporation of the residual solvent and follow-up the cyclization reaction at around 140°C . The progress of dynamic heating cyclization process is evidenced by the appearance of two maxima in the $\tan \delta$ curve: one at 170°C (corresponding to the T_g of poly(amidic acid)) and the other one at 282°C . The last maximum in $\tan \delta$ curve may be ascribed to the final T_g of the cyclized polymer. Regarding the polymer sample **B** (isothermal curing at 150°C) and polymer sample **D** (isothermal curing at 210°C), two maxima may be observed in the $\tan \delta$ curves which denote that the imidization process is not complete. The former maximum moves, as it was also reported by other authors [32], to higher temperatures as the curing temperature is increased. The latter maximum appears in all cases around the same range of temperature (275 – 288°C). Regarding the polymer sample **F**, the imidization conversion is high and the $\tan \delta$ curves shows only one peak when the curing temperature is raised to 250 – 260°C (Table 3).

Contact angle measurements

In order to measure the water dynamic contact angles the tensiometric method was used. The obtained values are presented in Table 4. Due to the presence of polar carboxylic acid (COOH) and amide (CONH) groups, the poly(amidic acid)s present much more polar surface than the corresponding polyimides. Usually, polyamidic acids imidized in situ by thermal treatment at elevated temperatures and the degree of imidization increases with cure temperature. Both the degree of imidization and the contact

Table 3 Glassy elastic modulus and transitions in the samples C, D, E, and F

Polymer samples	$E' \times 10^{-9}/\text{Pa}$ (25 °C)	$T_g/^\circ\text{C}$		T_g (tan δ)/ $^\circ\text{C}$	
		E' onset	E'' peak	First peak	Second peak
C	0.65	166	183	201	280
D	1.2	168	188	217	286
E	2.8	170	206	219	287
F	3.54	243	261	–	288

**Fig. 7** Tan δ curves of the polymer samples A, B, D, and F

angle values on the films increase with the cure temperature, as it is shown in Table 4. This reflects a decrease in the surface polarity due to the conversion of polar PAA to less polar polyimide film with increasing cure temperature [33, 34].

Dielectric characterization

Electroinsulating properties of these polymers have been also evaluated on the basis of dielectric constant values. The dielectric constant values can give valuable informations about the degree of imidization of the polymer samples. In general, the dielectric permittivity of a material is a complex quantity which consists of a real part (ϵ'), called “dielectric constant”, and an imaginary part (ϵ''), named “dielectric loss”. The magnitude of the dielectric constant is dependent upon the ability of the polarizable units to orient fast enough to keep up with the oscillation of the alternative electric field [35, 36]. There are a number of factors affecting the dielectric properties of materials [37]. The dielectric constant of polymer is a function of the total polarizability, αT [38]. There are three components to the polarizability of a polymer [39]: (1) The electronic polarizability, αE , which results from electrons being displaced

Table 4 The water contact angle of the polymer samples A, C, D, E, F, and G

Polymer samples	Curing temperature/ $^\circ\text{C}$	Water contact angle advancing/receding/ $^\circ$
A	110 (240 min)	87.86/49.22
C	180 (40 min)	87.94/58.26
D	210 (40 min)	87.95/55.15
E	240–250 (40 min)	88.67/44.78
F	250–260 (100 min)	88.92/43.04
G	250–260 (270 min)	91.19/63.19

Table 5 Dielectric constant of the polymer samples A–F

Polymer sample	Temp./ $^\circ\text{C}$	Frequency/Hz					
		0.1	1	10	100	1000	10000
A	25	8.8	5.6	4.7	4.3	4.2	4.0
B	25	4.3	3.89	3.75	3.65	3.60	3.53
C	25	3.49	3.45	3.42	3.39	3.36	3.33
D	25	3.32	3.28	3.25	3.23	3.20	3.18
E	25	3.00	2.98	2.96	2.94	2.93	2.92
F	25	2.83	2.82	2.81	2.80	2.80	2.79

from their equilibrium positions about the nucleus; (2) atomic polarizability, αA , which results from nonsymmetrical displacement of one atom to another, and (3) orientational polarizability, αO , which results from a change in alignment of the permanent dipole moments in the polymer to that of an applied electric field by physical movement of the group associated with the dipole. The electronic and atomic components of the dielectric constant are generally much smaller than the orientational components of polarization of a polar molecule. An exception to this is with conjugated systems where electron displacement can take place over a larger area and substantially increases electronic polarizability.

A polyamic acid has much more polar surface than the corresponding polyimide, due to the presence of polar carboxylic (COOH) and amide (CONH) groups. In consequence, one expect a higher dielectric constant for partially imidized polymer samples. As can be seen in Table 5, the dielectric constant of the polymer films decreased with increasing the degree of imidization. Thus, the dielectric constant at room temperature and 10 kHz decreased gradually as the cure temperature was increased from 4.0 (polymer sample A) to 2.8 (polymer sample E), proving that as the imidization temperature increases, more amide groups cyclodehydrate to imide rings. In the same time, it can be seen that the dielectric constant decreases with increasing frequency more pregnant in the case of polymer sample with more polar groups (A, B).

Conclusions

The thermal treatment of the films made from a polyimide based on benzophenonetetracarboxylic dianhydride and 4,4'-diamino-3,3'-dimethyl diphenylmethane shows the followings:

As the cure proceeds, amide groups are consumed and their characteristic absorption bands disappear in FTIR spectra, while the relative intensities of the absorption bands characteristic to imide cycles grow.

In the second step, the cure temperature increase led to higher temperatures where the simultaneous cyclization with dehydration and evaporation of solvent take place as well as to the decrease of mass loss (from 15 to 2%). The starting of decomposition of polyimide does not depend in a large measure of the cure temperature, being in the range of 460–495 °C with a maximum decomposition rate in the range of 560–570 °C.

Dynamic mechanical analysis shows that the rigidity of the polymer samples increases with the curing temperature increase. The disappearance of the first maximum in $\tan \delta$ curve proves that the degree of imidization attains a maximum value.

The dielectric constants of the polymer samples decrease and the contact angles increase with increasing of the degree of imidization.

Acknowledgements The authors address warm thanks to Dr. M. Cristea for DMA analysis and to V. Musteata for dielectric measurements.

References

1. Sroog CE. Polyimides. *Prog Polym Sci.* 1991;16:561–694.
2. Gosh MK, Mittal KL. Polyimides fundamentals and applications. New York: Marcel Dekker; 1996.
3. Hasegawa M, Horie K. Photophysics, photochemistry, and optical properties of polyimides. *Prog Polym Sci.* 2001;26:259–335.
4. Hergenrother PM. The use, design, synthesis and properties of high performance/high temperature polymers: an overview. *High Perform Polym.* 2003;15:3–45.
5. Bruma M, Hamciuc E, Sava I, Hamciuc C, Damaceanu MD, Robison J. Compared properties of polyimides based on benzophenonetetracarboxylic dianhydride. *Rev Roum Chim.* 2003;48:629–38.
6. Rusu DR, Damaceanu MD, Bruma M. Comparative study of soluble poly(keto-naphthylimide)s. *Rev Roum Chim.* 2009;54:1015–22.
7. Tyan HL, Liu, YC, Wei KH. Thermally and mechanically enhanced clay/polyimide nanocomposite via reactive organoclay. *Chem Mater* 1999;11:1942–1947
8. Tyan HL, Liu, YC, Wei KH. Effect of reactivity of organics-modified montmorillonite on the thermal and mechanical properties of montmorillonite/polyimide nanocomposites. *chem mater*, 2001;13:222–226
9. Cheng CF, Cheng HH, Cheng PW, Lee YJ. Effect of reactive channel functional groups and nanoporosity of nanoscale mesoporous silica on properties of polyimide composite. *Macromolecules.* 2006;39:7583–90.
10. Yuen SM, Ma CCM, Lin YY, Kuan HC. Preparation morphology and properties of acid and amine modified multiwalled carbon nanotube/polyimide composite. *Compos Sci Technol.* 2007;67:2564–73.
11. Adamczak AD, Spriggs AA, Fitch DM, Awad W, Wilkie CA, Grunlan JC. Thermal degradation of high temperature fluorinated polyimide and its carbon fiber composite. *J Appl Polym Sci.* 2010;115:2254–61.
12. Tead SF, Kramer EJ, Russell TP, Volksen W. Ion beam analysis of the imidization kinetics of polyamic ethyl ester. *Polymer.* 1990;31:520–3.
13. Becker KH, Schmidt HW. Para-linked aromatic poly(amic ethyl ester)s: precursors to rodlike aromatic polyimides. 1. Synthesis and imidization study. *Macromolecules.* 1992;25:6784–90.
14. Stoffel NC, Chandra S, Kramer EJ, Volksen W, Russell TP. Forward recoil spectrometry study of the diffusion of PMDA/ODA-based poly(amic ethyl esters). *Polymer.* 1997;38:5073–8.
15. Shin TJ, Ree M. In situ infrared spectroscopy study on imidization reaction and imidization-induced refractive index and thickness variations in microscale thin films of a poly(amic ester). *Langmuir.* 2005;21:6081–5.
16. Shin TJ, Ree MJ. Thermal imidization and structural evolution of thin films of poly(4,4'-oxydiphenylene p-pyromellitic diethyl ester). *Phys Chem B.* 2007;111:13894–900.
17. Jou JH, Huang PT. Effect of thermal curing on the structures and properties of aromatic polyimide films. *Macromolecules.* 1991;24:3796–803.
18. Saeed MB, Zhan MS. Effects of monomer structure and imidization degree on mechanical properties and viscoelastic behavior of thermoplastic polyimide films. *Eur Polym J.* 2006;42:1844–54.
19. Sava I. Synthesis and study of some aromatic polyimides based on 3,3'-dimethyl-4,4'-diaminodiphenylmethane. *Mater Plast.* 2006;43:15–9.
20. Sava I, Chisca S, Bruma M, Lisa G. Comparative study of aromatic polyimides containing methylene units. *Polym Bull.* 2010;65:363–75.
21. Lu QH, Yin J, Xu HJ, Zhang JM, Sun LM, Zhu ZK, Wang ZG. Preparation and properties of organo-soluble polyimides based on 4,4'-diamino-3,3'-dimethyldiphenylmethane and conventional dianhydrides. *J Appl Polym Sci.* 1999;72:1299–304.
22. Thomson B, Park Y, Painter PC, Snyder RW. Hydrogen bonding in poly(amic acid)s. *Macromolecules.* 1989;22:4159–66.
23. Gonzalo B, Vilas JL, Brezowski T, Perez-Jubindo MA, De La Fuente MR, Rodríguez M, Leon LM. Synthesis, characterization and thermal properties of piezoelectric polyimides. *J Polym Sci A.* 2009;47:722–30.
24. Snyder RW, Thomson B, Bartges B, Czerniawski D, Painter PC. FTIR studies of polyimides: thermal curing. *Macromolecules.* 1989;22:4166–72.
25. Shin TJ, Lee B, Youn HS, Lee KB, Ree M. Time-resolved synchrotron X-ray diffraction and infrared spectroscopic studies of imidization and structural evolution in a microscaled film of PMDA-3,4'-ODA poly(amic acid). *Langmuir.* 2001;17:7842–50.
26. Ojeda JR, Mobley J, Martin DC. Physical and chemical evolution of PMDA-ODA during thermal imidization. *J Polym Sci B.* 1995;33:559–69.
27. Kotera M, Nishino T, Nakamae K. Imidization processes of aromatic polyimide by temperature modulated DSC. *Polymer.* 2000;41:3615–9.
28. Shin TJ, Ree M. Poly(3,4'-oxydiphenylene pyromellitic acid), 1 time-resolved infrared spectroscopic study of thermal imidization in thin films. *Macromol Chem Phys.* 2002;203:791–800.
29. Komalan C, George KE, Kumar PAS, Varughese KT, Thomas S. Dynamic mechanical analysis of binary and ternary polymer

- blends based on nylon copolymer/EPDM rubber and EPM grafted maleic anhydride compatibilizer. *Express Polym Lett.* 2007;1: 641–53.
30. Cristea M, Gheorghiu-Ionita D, Bruma M, Simionescu BC. Thermal behavior of aromatic polyamic acids and polyimides containing oxadiazole rings. *J Therm Anal Calorim.* 2008;93: 63–8.
 31. Cristea M, Gaina C, Gheorghiu-Ionita D, Gaina V. Dynamic mechanical analysis on modified bismaleimide resins. *J Therm Anal Calorim.* 2008;93:69–76.
 32. Chiu HT, Cheng JO. Thermal imidization behavior of aromatic polyimides by rigid-body pendulum rheometer. *J Appl Polym Sci.* 2008;108:3973–81.
 33. Zuo M, Takeichi T, Matsumoto A, Tsutsumi K. Surface characterization of polyimide films. *Colloid Polym Sci.* 1998;276: 555–64.
 34. Paek SH. Effects of thermal imidization and annealing on liquid crystal alignment over rubbed polyimide layers: change in the pretilt angle. *Korea Polym J.* 2001;9:303–12.
 35. Deligoz H, Yalcinyuva T, Ozgumus S, Yildirim S. Electrical properties of conventional polyimide films: effects of chemical structure and water uptake. *J Appl Polym Sci.* 2006;100:810–8.
 36. Hamciuc C, Hamciuc E, Ipate AM, Okrasa L. Copoly(1,3,4-oxadiazole-ether)s containing phthalide groups and thin films made therefrom. *Polymer.* 2008;49:681–90.
 37. Mercer FW, Goodman TD. Effect of structural features and humidity on the dielectric constant of polyimides. *High Perform Polym.* 1991;3:297–310.
 38. Hougham G, Tesoro G, Shaw J. Synthesis and properties of polyimides made from perfluoro aromatic diamines. *J Polym Mater Sci Eng.* 1989;61:369–77.
 39. Hamciuc C, Hamciuc E, Bacosca I, Olariu M. Thermal and electrical properties of some poly(ether-imide) thin films. *Mater Plast.* 2010;47:11–5.